

# Field Measurements of Bubbles Injected by Breaking Waves

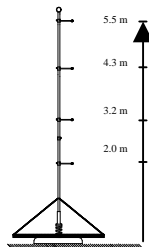
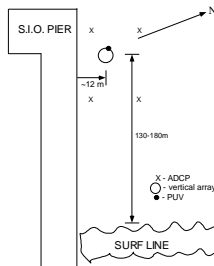
Eric J. Terrill and W. Kendall Melville  
Scripps Institution of Oceanography  
La Jolla, CA 92093-0230



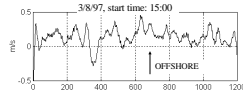
## INTRODUCTION.

Acoustical techniques for *in-situ* measurements of bubbles allows for robust field measurements under a wide range of environmental conditions. Bubbles will significantly modify the acoustical properties of water by scattering, dispersing, and attenuating incident sound waves. A recently developed technique which uses broadband acoustic pulse propagation (frequency band of 4kHz - 100 kHz) across a fixed pathlength allows for the direct measurement of the sound speed and attenuation at ping rates of a few Hz. The resulting acoustic data can be inverted using either a resonant approximation method (Wild 1946, Clay and Medwin 1979) or a finite-element method which corrects for off-resonant contributions to the attenuation (Commander & McDonald 1991). The ability to rapidly measure the acoustical properties of the bubbly medium allows the investigator to resolve the bubble size distributions with high temporal resolution.

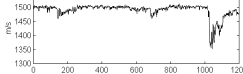
## SHALLOW WATER MEASUREMENTS



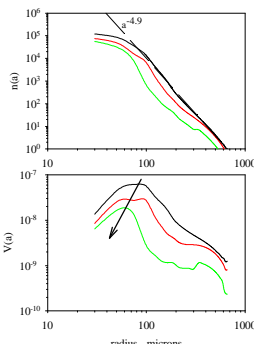
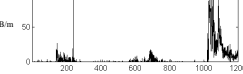
Measurements of bubbles were made north of the Scripps Pier in early March, 1997, using a vertical array of four of the broadband modules. At distances of O(100) m offshore the surfline, significant concentrations of bubbles were found to be advected offshore by rip currents. Below is a twenty minute time series of the offshore velocity measured near the vertical array using an electromagnetic current meter (orbital velocities of the waves have been filtered out) as well as the 4kHz sound speed and the 43 kHz attenuation measured at a depth of 1.1 m. The time series show the acoustic events correlating with periods of offshore flow as a result of the offshore transport of the bubbles.



4 kHz Sound Speed



43 kHz Attenuation



The mean bubble size distribution measured during the rip current event that starts near  $t = 1000$  seconds is shown at the left for three depths. The distributions appear to follow a power law relationship with a slope of approximately -5 for radii larger than 100 microns. Also shown is the corresponding volume contribution curves for the three distributions. The curves reveal that the radius which contributes most to the total void fraction is depth dependent and ranges from 60 - 90 microns.

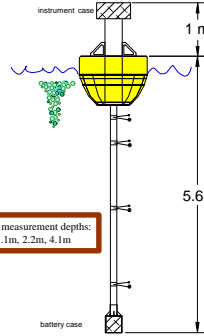
**Important for underwater acoustics.**  
The resonant frequency of the bubble whose radius contributes the most to the total void fraction corresponds to the frequency of maximum attenuation.

Volume contribution found by scaling size distribution by each bubble's volume  
 $V(a) = 4/3\pi a^3 n(a)$

## DEEP WATER MEASUREMENTS



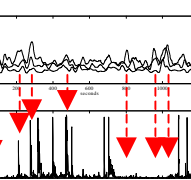
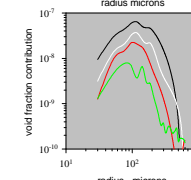
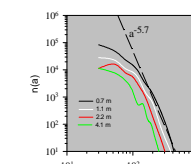
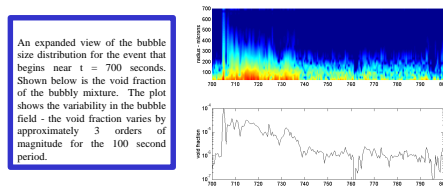
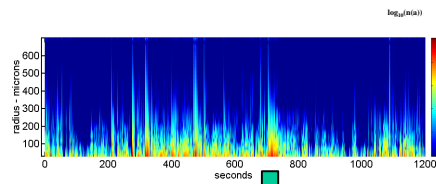
Four of the broadband acoustic modules were incorporated into a lightweight buoy package and deployed in a freely drifting mode off Point Conception, California in June, 1997. Bubble size distributions and the vertical temperature structure were measured at 2 Hz and 5 Hz respectively. Bubble densities were found to vary several orders of magnitude as a result of the instrument drifting into bubble clouds formed by breaking waves.



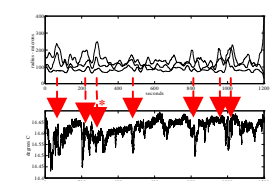
Bubble measurement depths:  
0.7m, 1.1m, 2.2m, 4.1m

Thermistor chain depths:  
0.7 m  
0.9 m  
1.3 m  
1.6 m  
2.2 m  
2.6 m  
3.4 m  
4.1 m

A 20 minute time series of the bubble size distribution measured at a depth of 0.7 m in wind speeds of 15 m/s and significant wave heights of 3.2 m. The logarithm of the bubble density, in units of number bubbles/m<sup>3</sup>/μm increment, is mapped to the color scheme shown. The bubble densities are highly variable due to intermittent wave breaking.



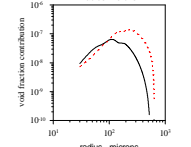
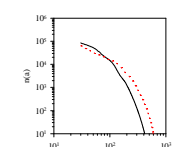
20 minute record of the peak in the volume contribution curves for the top three measurement depths (0.69 m, 1.3 m, 2.2 m) and the void fraction measured at the shallowest depth



time series of the radius at the peak in the volume contribution curves and the temperature measured at 4.1 m

example of two bubble size distributions during and not during a period of anomalous temperature

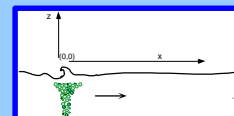
solid line - without anomaly  
dashed line - during anomaly



The mean bubble size distributions measured with the four modules are shown above for this event. The distributions exhibit power law behavior for radii greater than 100μm. Also evident is the trend of the radius which contributes to the most to the void fraction shifting to smaller values with depth.

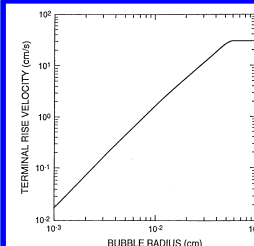
Simple advection-diffusion models can be used to explain several of the features observed in the rip current bubble size distributions.

$$\frac{\partial c}{\partial t} + U \frac{\partial c}{\partial x} + w_0 \frac{\partial c}{\partial z} = K_v \frac{\partial^2 c}{\partial z^2}$$

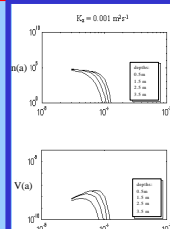
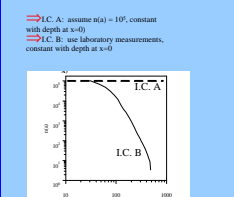


$U$  - velocity of rip current, assumed to be uniform (measured)  
 $w_0$  - rise velocity of bubbles (Thorpe 1982, Keeling 1993)  
 $K_v$  - eddy diffusivity, estimated from surf-zone measurements of turbulence using laser velocimetry (George, Pick & Garcia 1994) in range from  $O(10^7) - O(10^9) m^2 s^{-1}$   
equation simplified by neglecting bubble gas dissolution and bubble breakup (assumed small)

Two different initial conditions tried in model



Typical rise velocities of dirty bubbles (from Keeling, 1993).



Vertical dependence of peak radius: model and data  
The results emphasize the role of turbulent mixing and the depth dependence of the peak radius.

Model and data normalized by their values at the shallowest depth

Example of the model output of bubble size distribution and its corresponding volume contribution curve at a distance 100m offshore the surfline using initial condition B) and an eddy diffusivity of  $K_v = 10^{-3} m^2 s^{-1}$ .

